TLR ligand-induced podosome disassembly in dendritic cells is ADAM17 dependent

West, Michele A.; Prescott, Alan R.; Chan, Kui Ming; Zhou, Zhongjun; Rose-John, Stefan; Scheller, Juergen; Watts, Colin

Published in:
Journal of Cell Biology

DOI:
10.1083/jcb.200801022

Publication date:
2008

Document Version
Publisher's PDF, also known as Version of record

Published September 1, 2008

TLR ligand–induced podosome disassembly in dendritic cells is ADAM17 dependent

Michele A. West,[1] Alan R. Prescott,[1] Kui Ming Chan,[2] Zhongjun Zhou,[2] Stefan Rose-John,[3] Jürgen Scheller,[3] and Colin Watts[1]

[1]Division of Cell Biology and Immunology, Wellcome Trust Biocentre, College of Life Sciences, University of Dundee, Dundee DD1 5EH, Scotland, UK
[2]Department of Biochemistry, Li Ka Shing Faculty of Medicine, the University of Hong Kong, Pokfulam, Hong Kong
[3]Institute of Biochemistry, Christian Albrecht University, 24098 Kiel, Germany

Toll-like receptor (TLR) signaling induces a rapid reorganization of the actin cytoskeleton in cultured mouse dendritic cells (DC), leading to enhanced antigen endocytosis and a concomitant loss of filamentous actin–rich podosomes. We show that as podosomes are lost, TLR signaling induces prominent focal contacts and a transient reduction in DC migratory capacity in vitro. We further show that podosomes in mouse DC are foci of pronounced gelatinase activity, dependent on the enzyme membrane type I matrix metalloprotease (MT1-MMP), and that DC transiently lose the ability to degrade the extracellular matrix after TLR signaling. Surprisingly, MMP inhibitors block TLR signaling–induced podosome disassembly, although stimulated endocytosis is unaffected, which demonstrates that the two phenomena are not obligatorily coupled. Podosome disassembly caused by TLR signaling occurs normally in DC lacking MT1-MMP, and instead requires the tumor necrosis factor α–converting enzyme ADAM17 (a disintegrin and metalloprotease 17), which demonstrates a novel role for this "sheddase" in regulating an actin-based structure.

Introduction

Dendritic cells (DC) respond to microbial products by engaging in an activation program, which results in their progressive "maturation" and transformation from antigen-sampling cells to antigen-presenting cells (Guermonprez et al., 2002; Trombetta and Mellman, 2005; Wilson and Villadangos, 2005; Reis e Sousa, 2006). Maturation is typically triggered by ligation of Toll-like receptors (TLRs), and is accompanied and for the most part preceded by a variety of changes in DC morphology and behavior (Trombetta and Mellman, 2005; Watts et al., 2007). Within 30–60 min of TLR stimulation in vitro, DC redeploy their actin cytoskeleton to enhance antigen capture (West et al., 2004) and reorganize their vacuolar compartments to direct class II major histocompatibility complex (MHC) molecules to the cell surface (Kleijmeer et al., 2001; Chow et al., 2002; Boes et al., 2003). Here, they accumulate because of a cessation of ubiquitination and endocytosis of the class II MHC β chain (Shin et al., 2006; van Niel et al., 2006). Enhanced acidification of the endocytic pathway permits processing of the previously captured antigen and optimizes class II MHC peptide loading (Trombetta et al., 2003). In addition, newly synthesized proteins are ubiquitinated and accumulated in structures known as DALIs (dendritic cell aggresome-like induced structures; Lelouard et al., 2002). Location-specific TLR signaling, e.g., within phagosomes, leads to distinct organelle-autonomous changes, including accelerated phagosome maturation and enhanced presentation of antigens resident within the phagosome (Blander and Medzhitov, 2004; Blander and Medzhitov, 2006).

These changes can be viewed as adaptations that boost the performance of DC as antigen-capturing, -processing, and -presenting cells. For example, transiently enhanced antigen capture at the time and place of microbial product sensing should increase the display of pathogen-derived peptides to T cells. Consistent with this, simultaneous exposure of DC to antigen and TLR ligand led to enhanced T cell stimulation compared with

Correspondence to Colin Watts: c.watts@dundee.ac.uk

Abbreviations used in this paper: ADAM17, a disintegrin and metalloprotease 17; BMDC, bone marrow DC; CFSE, carboxyfluorescein succinimidyl ester; DC, dendritic cells; LPS, lipopolysaccharide; MHC, major histocompatibility complex; MMP, matrix metalloprotease; MT1-MMP, membrane type I MMP; PGE_2, prostaglandin E_2; SDC, spleen DC; TLR, Toll-like receptor; TNF-α, tumor necrosis factor α; WASp, Wiskott-Aldrich syndrome protein; WIP, WASp-interacting protein.

The online version of this article contains supplemental material.

Supplemental Material can be found at:
http://jcb.rupress.org/content/suppl/2008/09/08/jcb.200801022.DC1.html

The Rockefeller University Press $30.00
J. Cell Biol. Vol. 182 No. 5 993–1005
www.jcb.org/cgi/doi/10.1083/jcb.200801022

Published September 1, 2008

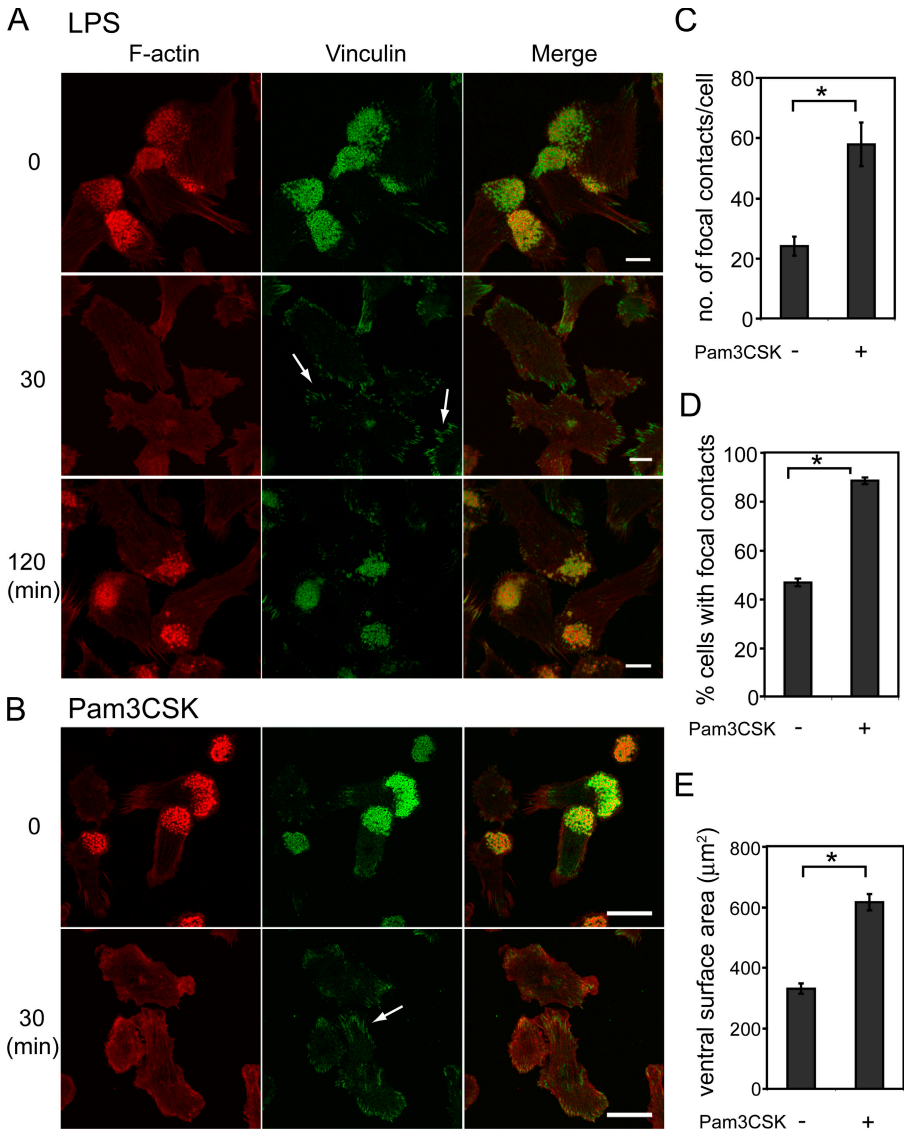

Figure 1. **TLR-signaling induces an increase in cell spreading and a switch from podosomes to focal contacts.** SDC were treated with 50 ng/ml LPS (A) or 100 ng/ml Pam3CSK (B) for the times indicated, then stained for F-actin (red) and vinculin (green). Arrows indicate focal adhesion–like contacts. The number of focal contacts per cell (C), the percentage of cells with focal contacts (D), and the ventral cell surface area of each cell (E) were quantitated from confocal images of untreated cells and cells treated with 100 ng/ml Pam3CSK for 30 min. Approximately 50 cells for each condition were quantitated for C. At least 450 cells for D and 120 cells for E for each condition, from three experiments performed on independent DC cultures, were scored. Data are means ± SEM. *, $P < 0.005$. Bars: (A) 10 μm; (B) 20 μm.

sequential exposure to first antigen and then TLR ligand (West et al., 2004). The possible significance of other rapid morphological changes triggered by TLR signaling is less obvious, however. In particular, we observed that TLR ligand–enhanced macropinocytosis was accompanied by a striking loss of F-actin–rich podosomes. As the rate of macropinocytosis subsequently fell, podosomes were reassembled, which suggested a reciprocal relationship and possibly a redeployment of cytoskeletal resources from podosomes to actin-rich ruffles and macropinosomes (West et al., 2004). Podosomes were also lost when human DC were stimulated with the TLR4 ligand lipopolysaccharide (LPS), but on a longer time scale compared with mouse DC (Burns et al., 2004; van Helden et al., 2006).

The biological significance of TLR ligand–induced podosome disassembly and, indeed, the biological functions of podosomes generally, are still uncertain. Podosomes have a striking morphology and are found in cells derived from the monocyte lineage, including osteoclasts, macrophages, and DC, as well as in endothelial cells and Src- and Rsv-transformed fibroblasts (Linder and Aepfelbacher, 2003; Buccione et al., 2004; Linder, 2007; Saltel et al., 2008). Podosomes are related to invadopodia found in invasive tumor cells, although the cellular and extracellular factors that induce one as opposed to the other structure are unclear. Podosomes consist of a core of F-actin and actin-regulatory proteins typically surrounded by a ring or matrix of other proteins, including integrins, paxillin, vinculin, and talin (Linder and Aepfelbacher, 2003). Many other proteins have been localized to podosomes, including, at least in osteoclasts and endothelial cells, matrix metalloproteases (MMPs). Several different MMPs have been reported to localize to podosomes and to invadopodia and, particularly in the latter, are responsible for localized degradation of the adjacent matrix (Linder, 2007). The F-actin core of podosomes turns over rapidly ($t_{1/2} = \sim 30$ s), and individual podosomes have short lifetimes of a few minutes (Destaing et al., 2003; Evans et al., 2003). Podosomes and invadopodia have been suggested to be involved in cell migration and invasion (Linder and Aepfelbacher, 2003; Buccione et al., 2004; Linder, 2007). For this reason, the presence of podosomes in DC and their acute regulation by TLR signaling is of considerable interest.

Published September 1, 2008

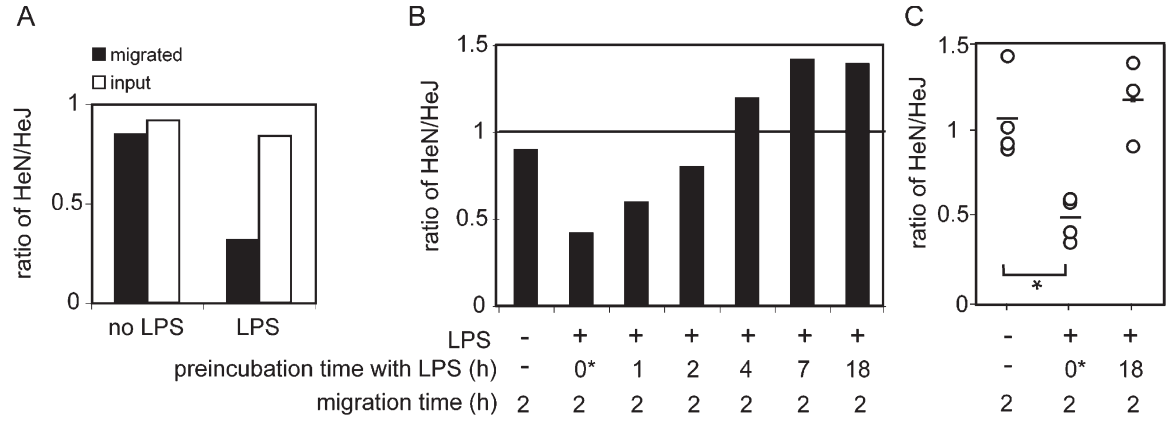

Figure 2. **LPS stimulation of DC transiently inhibits migration.** (A) BMDC from C3H/HeN and C3H/HeJ mice were labeled with CFSE or CMTMR, mixed in equal numbers with or without 50 ng/ml LPS, and added either into Transwell inserts or directly into control (input) wells. After 2 h at 37°C, migrated or input cells were recovered from the wells, quantitated by flow cytometry, and expressed as ratios of migrated or input HeN/HeJ. (B) DC were pretreated with 100 ng/ml LPS for different lengths of time before addition into the Transwell insert. Note that time = 0* data were obtained from cells where LPS was added immediately before the cells were placed onto the filter. Subsequent migration was for 2 h in all cases. The line indicates the 1:1 ratio achieved where HeN and HeJ migrate with equal efficiency. (C) Data from experiments on three or four independent DC cultures are shown. Bars represent mean data. *, $P < 0.05$.

Here, we investigate the significance and mechanism of reversible TLR ligand–induced disassembly of podosomes in mouse DC. Our results are consistent with the idea that DC migration and antigen sampling may be mutually exclusive activities, and they support the proposal that podosomes and specific podosome-localized MMP activities contribute to DC emigration from tissues. Membrane type I MMP (MT1-MMP) and, unexpectedly, a disintegrin and metalloprotease 17 (ADAM17) are involved in distinct aspects of DC podosome function and regulation.

Results

TLR signaling induces a switch from podosomes to focal contacts in DC

DC cultured from mouse bone marrow (BMDC) or spleen (SDC) form podosomes within 15 min of cell substrate contact. Podosomes are differentiated from other adhesive structures in fixed cells by their characteristic "bull's eye" appearance when stained with phalloidin to reveal the F-actin core and antibodies against other components such as vinculin, which are found in the surrounding ring (Fig. 1 A; Linder and Aepfelbacher, 2003). Exposure of mouse DC to TLR ligands induced the rapid but transient disassembly of podosomes (Fig. 1 A), and as we showed previously, a striking increase in membrane ruffling and macropinocytosis (West et al., 2004 and Video 1, available at http://www.jcb.org/cgi/content/full/jcb.200801022/DC1). Interestingly, vinculin (and other components of the podosome ring) became localized to focal contacts. These appeared longer and more numerous in LPS- (Fig. 1 A) or Pam3CSK- (a TLR2 ligand; Fig 1 B) treated DC. We quantitated the number of focal contacts for Pam3CSK-treated cells and found an approximately twofold increase after TLR ligand exposure (Fig. 1 C). In addition, the number of cells displaying focal contacts was also significantly increased (Fig. 1 D), and TLR ligand treatment increased the ventral surface area (i.e., footprint) of DC almost twofold (Fig. 1 E). Thus, TLR signaling induced a cell spreading response in addition to the previously described membrane ruffling and endocytosis response (West et al., 2004). A similar increase in DC surface area after LPS treatment has been observed by others (Granucci et al., 1999), and during revision of this work, van Helden et al. (2008) found that prostaglandin E_2 (PGE_2) induces a similar switch from podosomes to focal contacts in human monocyte–derived DC. 2 h after LPS stimulation, when podosomes reassembled, prominent focal contacts had largely disappeared (Fig. 1 A). Thus, in response to TLR stimuli, DC switch the type of adhesive structure found at the cell–substrate interface; before and after the phase of acute antigen sampling (West et al., 2004), podosomes are prominent, whereas during enhanced endocytosis, prominent focal contacts form.

DC transiently lose migratory capacity in vitro after TLR signaling

Although focal contacts are observed in migrating cells, prominent structures of the type we observed in LPS-stimulated DC correlate with an inhibitory effect on cell migration (Ridley et al., 2003). Moreover, because podosomes are proposed to be involved in cell migration, we wondered if DC might experience a transient loss of migratory capacity after TLR signaling. In other words, migration might be suppressed during the short phase of accelerated antigen capture. To test this, we performed short-term DC migration experiments in vitro after LPS challenge. Because the phase of DC spreading and the switch from podosomes to focal contacts only lasts ~90 min, we kept the time allowed for migration as short as possible. We found that ~5–10% of DC migrated through a Transwell chamber in 2 h. We avoided the use of chemokine attractants because the expression of chemokine receptors changes after TLR signaling (Sallusto and Lanzavecchia, 2000). To internally control the experiment, we included DC from both C3H/HeN and C3H/HeJ mice. The latter do not respond acutely to LPS because of a point mutation in TLR4 (Poltorak et al., 1998). Consequently, C3H/HeJ DC show no stimulation of pinocytosis, nor do they show any podosome loss in response to LPS (Fig. S1, available at http://www.jcb.org/cgi/content/full/jcb.200801022/DC1). We labeled BMDC from C3H/HeJ and

Published September 1, 2008

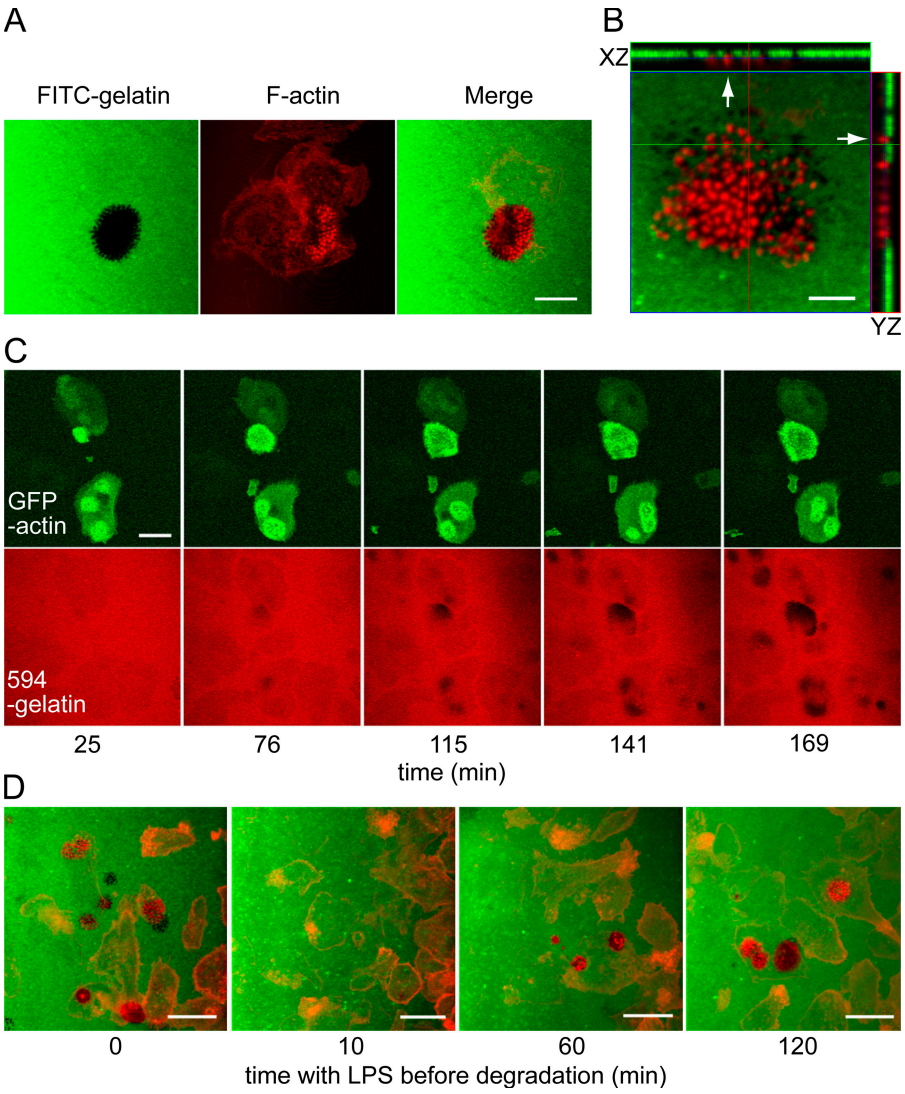

Figure 3. **DC podosomes degrade extracellular matrix.** (A) SDC were plated onto thin layers of cross-linked FITC-gelatin for 4 h and fixed, then podosomes were stained with TRITC-phalloidin. (B) xz and yz sections through a z series of confocal images revealed precise coincidence between individual podosomes and holes in the matrix (arrows). (C) BMDC infected with a GFP-actin–expressing retrovirus were plated onto Alexa 594–gelatin, and confocal images were collected every 2 min over a 220-min period. Images from individual time points of Video 2 (available at http://www.jcb.org/cgi/content/full/jcb.200801022/DC1) are shown. (D) SDC were treated with 50 ng/ml LPS for 10, 60, or 120 min before plating on FITC-gelatin for a further 2 h. Bars: (A and C) 10 µm; (B) 5 µm; (D) 20 µm.

from LPS-responsive C3H/HeN mice with different fluorescent dyes, mixed them in a 1:1 ratio, and placed them in the top half of Transwell chambers. The cells were exposed to LPS immediately before their transfer to the Transwell. After a 2 h period, cells that had migrated to the lower chamber were recovered (see Materials and materials), quantitated by flow cytometry, and expressed as a ratio (HeN/HeJ). As shown in Fig. 2 A, almost threefold fewer LPS-sensitive HeN cells migrated compared with HeJ cells, which demonstrates that TLR signaling compromised the ability of the cells to migrate. We repeated the experiment over a longer time course of LPS treatment. As before, when migration was measured immediately after LPS challenge, substantially fewer HeN cells had migrated compared with HeJ cells (decreased HeN/HeJ ratio; Fig. 2, B and C). However, after longer LPS exposure, the HeN cells resumed their migratory activity, and the migration ratio returned to and in some experiments exceeded 1 (Fig. 2, B and C). Collectively, these experiments show that TLR-stimulated DC experience a transient loss of migratory capacity in vitro, which coincides with the phase of acute stimulation of antigen capture, cell spreading, and podosome loss.

DC podosomes are foci of MMP activity

Podosomes are thought to be involved in cell migration and invasiveness because of their highly dynamic behavior and location at the leading edge of cells such as macrophages (Evans et al., 2003; Linder and Aepfelbacher, 2003; Buccione et al., 2004). In addition, at least in osteoclasts and endothelial cells, MMP activity has been localized to podosomes (Linder, 2007). Whether DC podosomes also organize extracellular matrix–degrading activity is not known. To address this, we plated DC onto thin layers of FITC-labeled gelatin and, after incubation at 37°C, visualized both the location of podosomes and the integrity of the FITC-gelatin layer (Bowden et al., 2001). As shown in Figs. 3 A and S2 (available at http://www.jcb.org/cgi/content/full/jcb.200801022/DC1), discrete holes in the gelatin matrix were seen in the vicinity of F-actin– and vinculin-containing DC podosome clusters. At higher magnification, xz and yz section planes through a confocal z stack revealed that the holes in the FITC-gelatin matrix were frequently below F-actin–rich podosomes, which demonstrates that matrix degradation occurred specifically at podosome sites (Fig. 3 B). Holes in the gelatin matrix that did not coincide with F-actin presumably corresponded

Published September 1, 2008

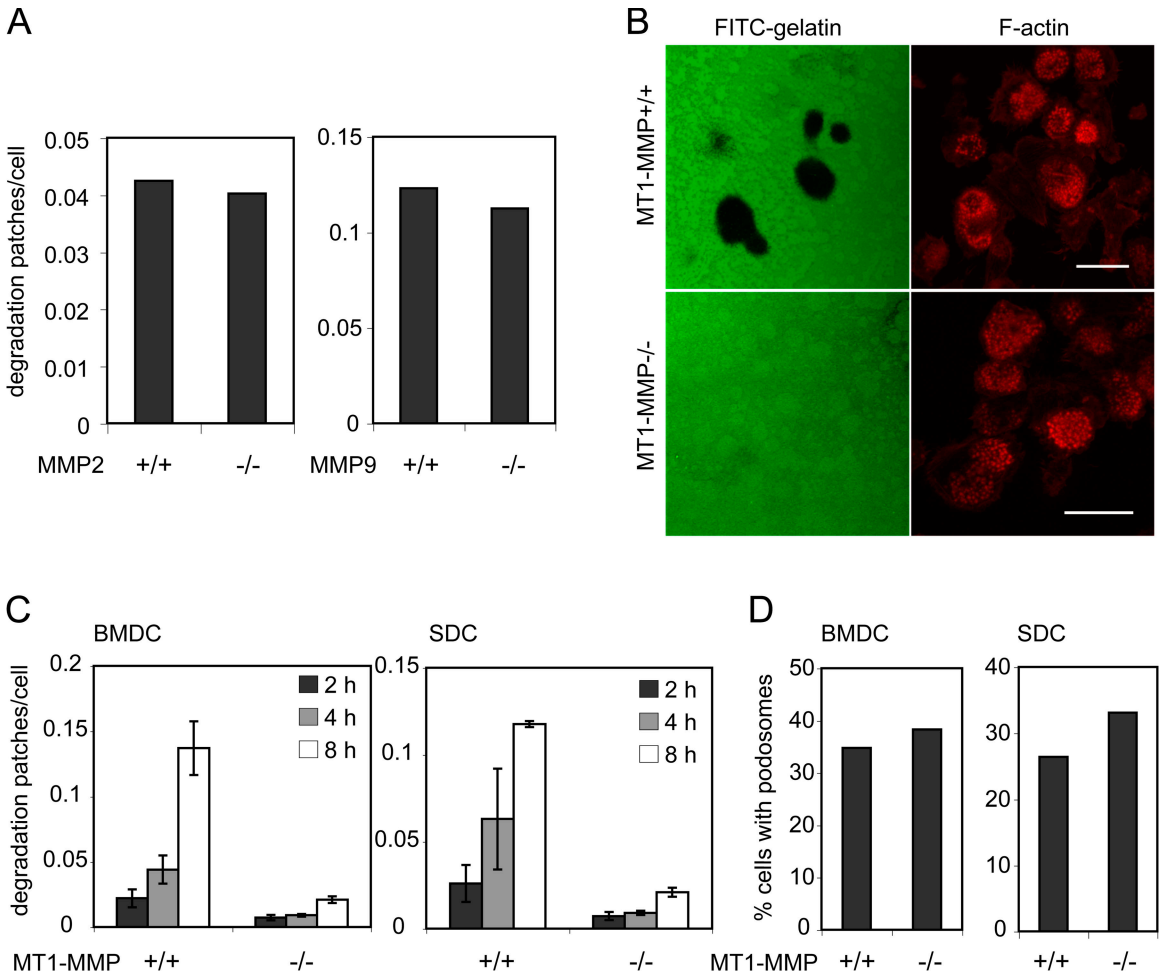

Figure 4. **MT1-MMP–deficient DC are unable to degrade matrix.** DC from wild-type or MMP-deficient mice were plated on cross-linked FITC-gelatin matrix for 4 h or for the times indicated, then fixed and stained with TRITC-phalloidin. (A) Quantitation of matrix degradation by DC from MMP2$^{-/-}$ and MMP9$^{-/-}$ mice. (B) Confocal images of MT1-MMP$^{+/+}$ and MT1-MMP$^{-/-}$ SDC plated on matrix. Bars 20 µm. (C) Quantitation of matrix degradation by MT1-MMP$^{+/+}$ and MT1-MMP$^{-/-}$ BMDC and SDC. Data are means of experiments performed on DC cultures from two mice of each genotype (error bars indicate the data range), and are representative of data from five MT1-MMP$^{-/-}$ mice in total. (D) The percentage of MT1-MMP$^{+/+}$ and MT1-MMP$^{-/-}$ BMDC and SDC with podosomes when plated on matrix.

to podosomes that had turned over during the time of the experiment. To gain further evidence that podosomes were responsible for the matrix-degrading activity of DC, we expressed GFP-actin via a retrovirus and followed both the dynamics of podosomes and matrix degradation over time. Fig. 3 C and Video 2 confirm that podosomes are highly dynamic structures in DC and that degradation occurs at podosome sites. The focused matrix degradation observed beneath DC podosomes is striking and more similar to what has been observed for invadopodial degradation, e.g., in carcinoma cells (Linder, 2007). Focused proteolysis beneath DC podosomes was also observed when the DC were plated on non-cross-linked gelatin, collagen, and fibronectin (Fig. S2).

Because podosomes are transiently lost after TLR stimulation, we predicted that matrix-degrading activity might be similarly affected. As with the migration studies, we kept the time allowed for matrix degradation to the minimum necessary in order to increase the resolution of the experiment. At different times after LPS exposure, DC were plated on FITC-gelatin and incubated for 2 h at 37°C. As predicted, DC lose the ability to degrade the gelatin matrix after LPS challenge but regain this capacity as podosomes returned (Fig. 3 D). Thus, matrix-degrading activity can be acutely regulated by TLR signaling in DC through reversible disassembly of podosomes. As expected, matrix degradation was caused by MMP activity because the broad-specificity MMP inhibitor GM6001, but not inhibitors of other protease classes or an inactive GM6001 analogue, blocked the appearance of degradation patches beneath DC (unpublished data).

MT1-MMP is responsible for the in vitro matrix-degrading activity of DC podosomes

To identify the GM6001-sensitive activity responsible for podosome-associated matrix degradation, we investigated which MMPs are expressed in cultured mouse DC and tested DC from mice lacking selected MMPs. MMPs 8, 9, 12, 13, 14, and 19 were all expressed in BMDC as determined by microarray experiments (unpublished data). In addition, quantitative PCR data indicated that cultured SDC additionally expressed MMPs 2, 3, and 28 (unpublished data). The presence of TGFβ during cell culture may account for the additional MMPs expressed in SDC. MMP2 or MMP9 are gelatinases, but neither were absolutely required

Published September 1, 2008

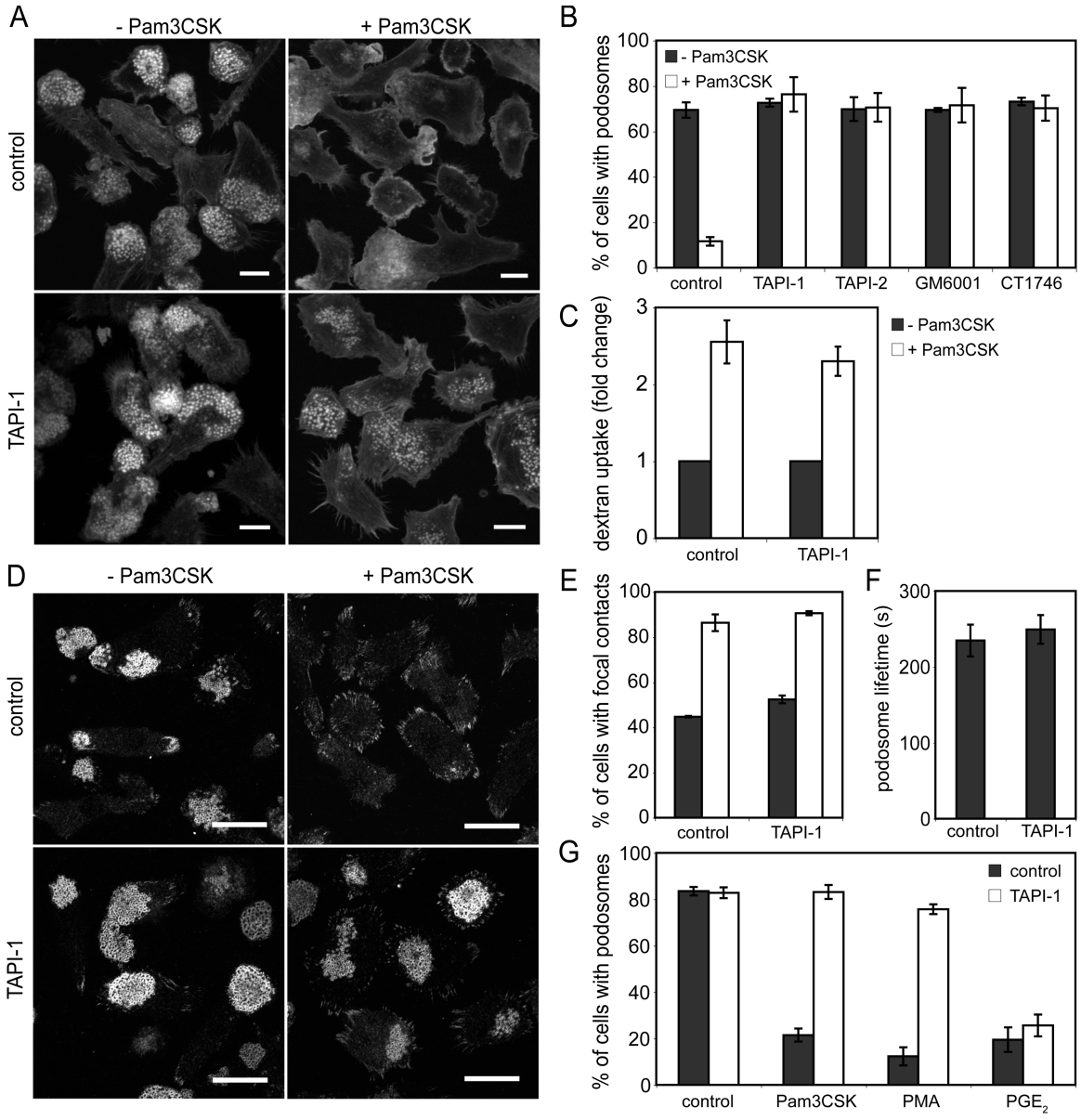

Figure 5. **MMP inhibitors block TLR signaling–induced podosome disassembly but not boosted pinocytosis or increased focal contacts.** SDC were pretreated with MMP inhibitors TAPI-1, TAPI-2, GM6001, or CT1746 (all at 25 μM) for 20 min before TLR stimulation for 30 min with 100 ng/ml Pam3CSK, then the cells were stained with TRITC-phalloidin to reveal podosomes. Representative confocal images (A) and quantitation of cells with podosomes (B) are shown. (C) SDC that had been pretreated with TAP-1 and stimulated with Pam3CSK as before were incubated with 1 mg/ml FITC-dextran for 10 min at 37°C, then pinocytosed dextran was measured by flow cytometry. The stimulated fold changes in dextran uptake are shown. (D) SDC were treated with TAPI-1 and Pam3CSK as before and stained for vinculin to reveal focal contacts. (E) Quantitation of cells with focal contacts. (F) The lifetimes of individual podosomes in untreated or TAPI-1–treated BMDC expressing GFP-actin were quantitated from time-lapse sequences, as described in Materials and methods. Between 160 and 760 podosome events per cell for 10 cells (from two independent DC cultures) per treatment were measured. (G) The effect of TAPI-1 pretreatment (as before) on podosomes in SDC stimulated with 100 ng/ml Pam3CSK, 30 ng/ml PMA, or 10 μg/ml PGE_2 for 30 min was quantitated after TRITC-phalloidin staining. Data are means ± SEM of experiments performed on DC from three (B, C, and E) or five mice (G). Bars: (A) 10 μm; (D) 20 μm.

because DC from mice lacking one or other of these MMPs showed no obvious defect in matrix degradation (Fig. 4 A). We also tested DC from mice lacking membrane-anchored MT1-MMP (MMP14) because this activity has been associated with invadopodia in invasive tumor cells (Nakahara et al., 1997). MT1-MMP–deficient mice are severely affected by the loss of this key MMP activity. They are not born at the expected Mendelian ratio, have multiple skeletal and connective tissue abnormalities, and die ∼2 wk after birth (Holmbeck et al., 1999; Zhou et al., 2000). We set up DC cultures from 10–14-d-old MT1-MMP–deficient mice alongside DC from wild-type littermates. The growth of DC in culture did not seem to be affected by the loss of MT1-MMP. However, compared with wild-type DC, gelatin matrix–degrading activity in the MT1-MMP–null DC was almost completely lost (Fig. 4 B). This striking result was observed in both BMDC and in SDC. Quantitation of the degradation of the underlying matrix confirmed that MT1-MMP–deficient DC are profoundly compromised in their ability to degrade a gelatin matrix, even over an 8-h time course (Fig. 4 C), although normal levels of podosomes were observed (Fig. 4 D).

Published September 1, 2008

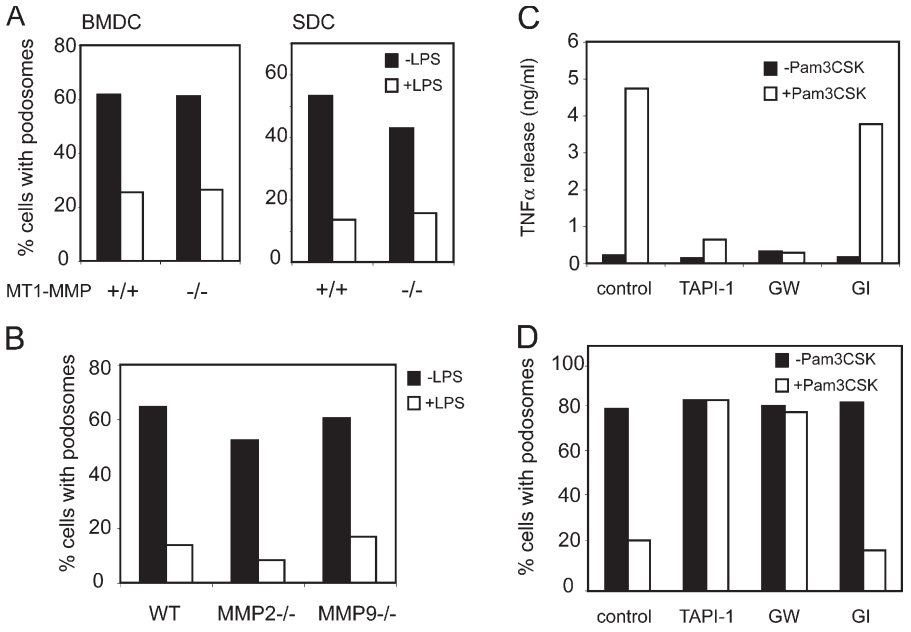

Figure 6. **TLR-induced podosome disassembly requires a distinct metalloprotease activity.** DC from MT1-MMP– (A) and MMP2- or MMP9- (B) deficient mice were fixed after LPS stimulation (50 ng/ml, 30 min) and stained with TRITC-phalloidin to allow assessment of podosome loss. SDC were pretreated for 20 min with 25 μM TAPI-1, 3 μM GW280264X (GW), or 3 μM GI254023X (GI), then stimulated with 100 ng/ml Pam3CSK. TNF-α shedding into the medium measured by ELISA (C) and quantitation of cells with podosomes (D) are shown. Data are representative of experiments performed on DC from at least two mice.

MMP inhibitors block TLR signaling–induced podosome disassembly

While we were testing different protease inhibitors for their effect on podosome-organized matrix-degrading activity, we made an unexpected observation: the presence of MMP inhibitors completely blocked TLR ligand–induced podosome disassembly. Four different MMP inhibitors (GM6001, TAPI-1, TAPI-2, and CT1746) all blocked this response (Fig. 5, A and B). Moreover, the concentrations of MMP inhibitors required to arrest this response were the same as those required to block a second TLR-induced and MMP-dependent response, the shedding of tumor necrosis factor α (TNF-α) from the DC surface (unpublished data). This finding allowed us to test the hypothesis that TLR ligand–stimulated macropinocytosis might be dependent on podosome disassembly, e.g., to release additional actin resources. Cultured mouse DC were stimulated with Pam3CSK in the presence or absence of TAPI-1, and macropinocytosis was measured by FITC-dextran uptake (West et al., 2004). In fact, blockade of podosome disassembly with the MMP inhibitor had little effect on LPS-stimulated endocytosis (Fig. 5 C). Furthermore, the presence of an MMP inhibitor had little effect on the TLR ligand–induced increase in prominent focal contacts (Fig. 5, D and E) or ventral cell surface area (not depicted). These results lead to two important conclusions. First, neither the stimulated endocytic response nor the increase in focal contacts and cell spreading is obligatorily coupled to the disassembly of podosomes. Second, MMP activity is not only organized at podosomes for purposes of matrix degradation but can additionally initiate podosome loss after TLR signaling.

The unexpected involvement of MMP activity in podosome stability in TLR ligand–stimulated cells raised the question of whether MMP activity also affected podosome lifetime under normal, i.e., non-TLR-stimulated, conditions. DC expressing GFP-actin were left untreated or treated with the MMP inhibitor TAPI-1. Podosomes were imaged by time-lapse microscopy, and kymographs of podosome clusters were analyzed to determine the lifetimes of individual podosomes (see Materials and methods and Fig. S3, available at http://www.jcb.org/cgi/content/full/jcb.200801022/DC1). Although there was some variation in podosome F-actin core lifetime, even within the same podosome cluster (Fig. S3), the distribution of lifetimes and the mean podosome lifetime was essentially the same with or without inhibition of MMP activity (Figs. 5 F and S3).

PGE_2 has been reported to rapidly induce podosome disassembly in human DC (van Helden et al., 2006), a finding we confirmed in mouse DC (Fig. 5 G). However, this response was insensitive to MMP inhibitors, demonstrating that TLR ligands and PGE_2 destabilize podosomes by distinct mechanisms. PMA also triggered podosome disassembly in DC and, similar to TLR-driven disassembly, this was also dependent on MMP activity (Fig. 5 G).

TLR-induced podosome disassembly requires a distinct MMP activity

We asked which MMP activities are required for TLR ligand–induced podosome disassembly. Interestingly, LPS induced loss of podosomes to the same extent in wild-type and in MT1-MMP–deficient DC, which indicates that matrix degradation and podosome stability are controlled by different MMP activities (Fig. 6 A). Furthermore, MMP2 and MMP9 were also ruled out because DC lacking these enzymes disassembled podosomes normally in response to LPS (Fig. 6 B). MMP activities might destabilize podosomes by proteolytic cleavage or "shedding" of key proteins, e.g., integrins, that mediate substrate attachment at podosomes. Such activities could be recruited and/or activated after TLR signaling. To further define the MMP activities responsible and test whether known sheddases such as ADAM17 (also known as TNF-α–converting enzyme [TACE]) and ADAM10 might be involved, we tested two additional selective inhibitors of these enzymes: GW280264X (GW), which blocks both ADAM10 and ADAM17; and GI254023X (GI), which inhibits ADAM10 100-fold more effectively than ADAM17 (Hundhausen et al., 2003;

Published September 1, 2008

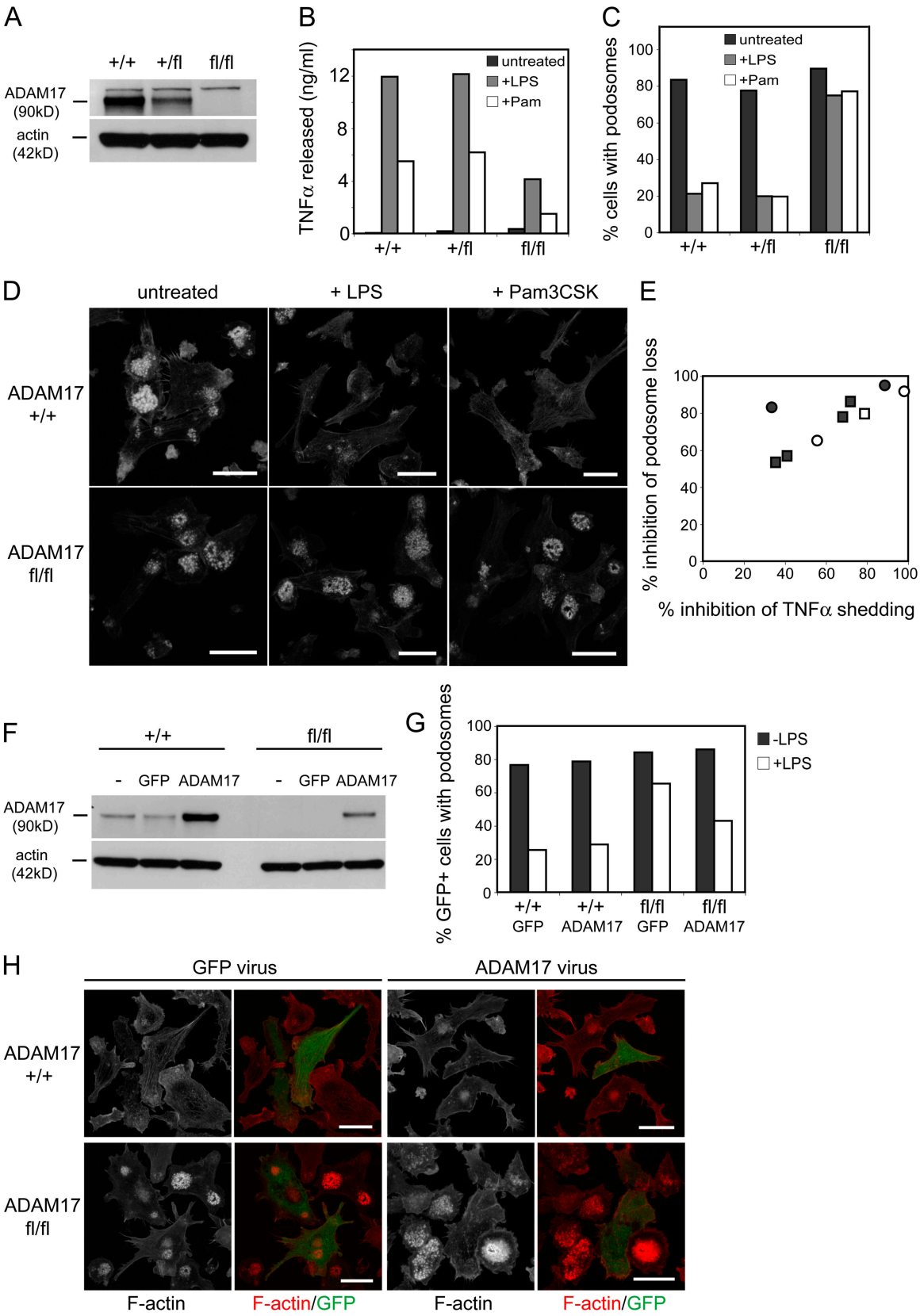

Figure 7. **ADAM17 is required for TLR-signaling induced podosome disassembly.** BMDC were cultured from ADAM17$^{+/+}$, ADAM17$^{+/fl}$, or ADAM17$^{fl/fl}$ mice. Lysates from these were immunoblotted with antibodies against ADAM17 or actin (loading control). (B) TNF-α, released by BMDC during treatment with 50 ng/ml LPS or 100 ng/ml Pam3CSK for 2 h, was measured by ELISA. (C) ADAM17$^{+/+}$, ADAM17$^{+/fl}$, or ADAM17$^{fl/fl}$ BMDC were stimulated with 50 ng/ml LPS or 100 ng/ml Pam3CSK for 30 min, then assessed, after staining with TRITC-phalloidin, for the presence of podosomes. (D) Confocal images of the cells quantitated in C confirm that the LPS- or Pam3CSK-stimulated podosome loss observed in ADAM17$^{+/+}$ cells is inhibited in ADAM17$^{fl/fl}$ cells.

Published September 1, 2008

Chalaris et al., 2007). TLR signaling is known to stimulate TNF-α release from its membrane-bound precursor form in an ADAM17-dependent manner (Black et al., 1997), providing a convenient assay for these inhibitors. As before, DC were stimulated with a TLR ligand (Pam3CSK) in the presence or absence of these inhibitors, and both TNF-α release and podosome loss were monitored. TNF-α release from the cells was potently inhibited by the GW compound but only slightly by GI, which is consistent with the known involvement of ADAM17 but not ADAM10 in stimulated TNF-α release (Fig. 6 C). Podosome loss closely mirrored this response, being blocked by GW but not by GI (Fig. 6 D), which is consistent with a possible involvement of ADAM17.

To investigate this further, we took advantage of a newly derived line of mice carrying two floxed alleles of ADAM17, which express low levels of the enzyme even in the absence of Cre-mediated excision, because of an aberrant splicing event. These ADAM17$^{fl/fl}$ mice, unlike ADAM17-null mice, are viable and will be fully described elsewhere (unpublished data). As shown in Fig. 7 A, levels of ADAM17 in BMDC expanded from the ADAM17$^{fl/fl}$ mice were substantially reduced compared with the wild type. As expected, the normal TLR ligand–induced shedding of TNF-α was also substantially reduced in DC from the ADAM17$^{fl/fl}$ mice (Fig. 7 B), although the actual deficit was variable among DC cultures generated from different mice. Importantly, DC from the ADAM17$^{fl/fl}$ mice showed a striking inability to disassemble podosomes in response to TLR signaling (Fig. 7, C and D). In DC from different mice, this ranged from virtually complete inhibition to ∼50% inhibition of the response. When we compared the percentage of inhibition of TLR-induced TNF-α release versus the percentage of inhibition of TLR-induced podosome loss in BMDC and SDC from five different ADAM17$^{fl/fl}$ mice, there was a positive correlation between the two (Fig. 7 E; r = 0.76). To confirm that ADAM17 activity was required for podosome disassembly, we attempted to rescue the response by reintroduction of ADAM17 into primary DC from the ADAM17$^{fl/fl}$ mice. As shown in Fig. 7 F, retroviral reexpression of ADAM17 restored protein levels in ADAM17$^{fl/fl}$ mouse DC. Importantly, when DC infected with the ADAM17 virus (GFP+) were stimulated with LPS, the podosome disassembly response was largely restored (Figs. 7, G and H). In contrast, neighboring uninfected (GFP−) cells retained their podosomes (Fig. 7 H). These data demonstrate, unexpectedly, that the TNF-α and L-selectin shedding enzyme ADAM17/TACE plays a key role in TLR-induced podosome regulation in mouse DC.

Discussion

When DC encounter innate immune stimuli such as TLR ligands, a spectrum of striking cell biological changes occur early in the overall maturation response. These include reorganizations of the actin cytoskeleton and the vacuolar system, which enhance antigen capture, processing, and presentation (for reviews see Trombetta and Mellman, 2005; Watts et al., 2007). We previously described an acute response characterized by two striking changes to the actin cytoskeleton: an up-regulation of membrane ruffling–driven macropinocytosis and a disappearance of F-actin–rich podosomes (West et al., 2004). Both changes were transient and occurred with the same kinetics. Fully mature DC have few podosomes (unpublished data; Burns et al., 2001), which indicates that they may have a specific role in the biology of immature DC. Here, we investigated further the TLR regulation of podosomes in immature DC.

Our data support the idea that DC transiently lose migratory capacity during acute antigen sampling. Migration through a transwell barrier was impeded after LPS challenge, as shown by the fact that when mixed populations of LPS responsive and nonresponsive DC were monitored, the responsive DC lagged behind. This lag phase coincided with a transient switch in the type of adhesive structure expressed by DC from predominantly podosomes to focal contacts. We suggest that the loss of migratory capacity is due, at least in part, to the loss of actin-rich podosomes and the development of more prominent focal contacts and cell spreading. The role of podosomes in cell migration on planar substrates as opposed to cell invasiveness is still debated. The presence of podosomes at the leading edge of macrophages (Evans et al., 2003) and DC (Burns et al., 2004; Svensson et al., 2008) suggests that they contribute to directed migration, but it is clear that podosomes are not essential for migration on 2D substrates. For example, human DC matured with LPS for 16 h lost podosomes, but their capacity to migrate on 2D surfaces was actually increased (van Helden et al., 2006), and macrophages deficient in Rac2 lacked podosomes but still migrated on a coated glass substrate (Wheeler et al., 2006). Nonetheless, considerable evidence implicates podosomes and invadopodia in cell migration in three dimensions, e.g., through an extracellular matrix barrier. MMP activity organized by podosomes and invadopodia is thought to be a key element in this process (Linder, 2007). Although no defined matrix barrier was used in our short-term migration experiments, podosomes may help the cell to negotiate the filter barrier. This may be because MMPs have additional roles besides pericellular matrix proteolysis that may also aid migration (Mott and Werb, 2004; Van Lint and Libert, 2007), e.g., cytokine and chemokine processing and shedding of cell surface proteins such as syndecan-1 (Endo et al., 2003) and CD44 (Nakamura et al., 2004). These additional MMP functions may be most effective when focused at the advancing cell boundary. We recently found that disruption of normal ARF6 GTPase activity strongly inhibited both podosome formation and immature DC migration in vitro, again linking these structures to DC migratory capacity (Svensson et al., 2008).

(E) The percent inhibition of podosome loss versus the percent inhibition of TNF-α shedding (relative to +/+ controls) for experiments performed on BMDC (squares) or SDC (circles), which had been treated with LPS (closed symbols) or Pam3CSK (open symbols), as before, from five ADAM17$^{fl/fl}$ mice. The Pearson coefficient for the data is 0.76. (F) Immunoblots of lysates from uninfected BMDC or BMDC infected with retrovirus expressing either GFP marker alone or GFP and ADAM17 show that expression of ADAM17 can be restored in ADAM17$^{fl/fl}$ cells. ADAM17$^{+/+}$ or ADAM17$^{fl/fl}$ BMDC infected with GFP or ADAM17 retrovirus were left untreated or stimulated with 50 ng/ml LPS for 30 min, then stained with TRITC-phalloidin. GFP^{+} (infected) cells from each condition were scored for the presence of podosomes (G), and representative confocal images of LPS-treated cells are shown (H). Bars, 20 μm.

Published September 1, 2008

How might the TLR ligand–induced loss and subsequent regain of podosomes be rationalized in the context of DC behavior in vivo? Under noninfectious resting conditions, DC are known to exit tissues at a basal rate and travel to lymphoid organs (Huang et al., 2000; Lanzavecchia and Sallusto, 2001). These constitutively migrating DC are believed to be important in the induction of tolerance to self-antigens (Heath and Carbone, 2001; Steinman et al., 2003). We propose that DC use podosomes or related structures as part of the machinery needed for DC mobilization and exit from tissues under these conditions (Fig. 8). Upon detection of an infectious or inflammatory stimulus, DC would initiate a transient phase of enhanced actin-dependent capture of local antigens that, we propose, may be facilitated by loss of migratory capacity as a result of a switch in the dominant adhesive structure, i.e., podosomes to focal contacts. At the end of this period of acutely stimulated endocytosis, podosomes may reform, and migration of antigen-loaded DC could resume (Fig. 8). The microbial and inflammatory stimuli encountered also serve to switch the DC from a tolerogenic to an immunogenic mode (Lanzavecchia and Sallusto, 2001; Reis e Sousa, 2006). Though obviously speculative, the model implies that DC undergo a transient loss of migratory capacity during the phase of acute antigen endocytosis, a prediction that is at least consistent with the in vitro experiments described here.

Podosomes have now been described in several cell types, and although there is abundant information on their composition, the factors that control their formation, lifetime, and function are still under investigation (Buccione et al., 2004; Linder, 2007; Saltel et al., 2008). Their acute response in DC to TLR stimuli provides a powerful system to investigate some of these questions. We show here that, as in osteoclasts and endothelial cells, DC podosomes organize pericellular proteolytic activity, and we show that a TLR stimulus transiently ablates this activity. This would also fit with the proposed loss of tissue-emigrating ability. Surprisingly, this gelatin matrix–degrading activity was caused by a single MMP, MT1-MMP. MT1-MMP is known to activate other MMPs such as MMP2. However, MMP2-deficient DC showed normal in vitro matrix degrading capacity, which suggests that MT1-MMP may be directly involved in pericellular proteolytic activity or activate a different MMP. The possible link between MT1-MMP and DC migration is intriguing, as this membrane-anchored MMP has been frequently associated with tumor cell invasiveness and metastasis in vivo (Sato et al., 2005). Assessing a role for MT1-MMP in DC migration in vivo is problematic because of the poor health and very short lifespan of the null mice and will require either conditional and/or DC-specific deletion for full investigation. However, DC migration through tissue and matrix barriers in vivo may well require more than a single MMP activity. For example, Langerhans cell emigration was deficient in skin explants from MMP9-deficient mice (Ratzinger et al., 2002). In the same study, the presence of tissue inhibitor of metalloprotease 2, which inhibits MT1-MMP and other MMPs but not MMP9, also inhibited Langerhans cell migration. As already noted, it has become clear that MMPs also process a variety of non-matrix substrates including chemokines, cytokines, and their receptors (Van Lint and Libert, 2007). It is therefore tempting to speculate that podosome-organized MMP activity may be important for DC processing of migratory cues that involve these additional substrates.

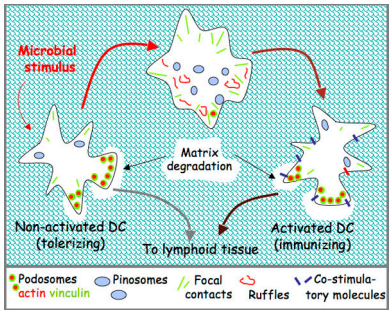

Figure 8. **Proposed relevance of TLR-regulated actin changes to DC biology in vivo.** DC migrate from peripheral tissues to lymph nodes under noninflammatory conditions using podosomes and their associated MMP activity as part of the migratory apparatus. Upon detection of a microbial stimulus, DC are proposed to enter a transient window of enhanced actin-driven antigen endocytosis, loss of podosomes, and appearance of prominent focal contacts, thus optimizing local antigen acquisition and suppressing migration. As endocytosis subsequently decreases, focal contacts are replaced by reappearing podosomes and migratory capacity is restored. Such DC conditioned by a microbial stimulus are potentially "immunizing" rather than "tolerizing."

We identified an unexpected and novel relationship between MMP activity and podosome genesis and stability. The presence of MMP inhibitors completely blocked TLR ligand–induced loss of podosomes. Interestingly, the relevant MMP activity was not MT1-MMP, as podosomes disassembled normally in LPS-treated DC from MT1-MMP–deficient mice, but rather was the TNF-α–converting enzyme ADAM17. To our knowledge this is the first time that this activity has been implicated in the dynamics of actin-based structures associated with cell adhesion and migration. The ADAMs family of proteinases contains the major cell surface sheddases known to cleave cytokines, growth factors, and their receptors, as well as adhesion molecules (Seals and Courtneidge, 2003). Moreover, shedding events such as the release of TNF-α by ADAM17 is known to be activated by TLR ligands in a MAP kinase–dependent fashion (Schlondorff and Blobel, 1999; Soond et al., 2005; Rousseau et al., 2008), which is consistent with our finding that TLR-triggered podosome disassembly is blocked by MAP kinase inhibitors (West et al., 2004).

The precise mechanistic link between ADAM17 and TLR ligand–triggered podosome disassembly remains to be elucidated. Most likely, TLR signaling induces the recruitment to the cell surface and/or activation of ADAM17, which then cleaves key surface proteins required for cell–substrate contact and podosome formation. The identity of these proteins remains to be established. Podosome reappearance may require the repopulation of the cell surface with those proteins. Recently, the intracellular protease calpain has also been implicated in podosome stability. Calpain inhibitors increased recruitment of integrins and Wiskott-Aldrich syndrome protein (WASp) to podosomes, apparently by blocking calpain-mediated cleavage of WASp (Calle et al., 2006). A follow-up study (Chou et al., 2006) showed that DC lacking WASp-interacting protein (WIP) also lack normal podosomes, as do WASp-deficient DC (Burns et al., 2004).

Published September 1, 2008

WIP appears to regulate both the location and stability of WASp and is localized in podosome actin cores (Chou et al., 2006). Interestingly, $WIP^{-/-}$ DC had more pronounced focal contacts and membrane ruffles compared with wild-type DC, which is similar to the state transiently induced by TLR signaling. However, we found that calpain inhibitors did not affect the sensitivity of DC podosomes to TLR signaling (unpublished data), which indicates that perturbation of the calpain–WASp–WIP system is not likely to be the primary target of LPS signaling. Apparently, both the calpain and MMP systems can influence podosome stability.

Having found a way to selectively inhibit part of the TLR ligand–induced cytoskeleton response, we were able to test the possibility that podosome disassembly might be necessary to fuel increased actin-dependent endocytosis. In fact, macropinocytosis was boosted to almost the same extent in the presence of MMP inhibitors, which demonstrates that the two phenomena are coincident but not obligatorily linked. DC evidently have sufficient actin cytoskeletal resources to maintain significant numbers of podosomes and to develop the pronounced ruffles that give rise to macropinosomes.

In summary, in spite of the increasing attention that podosomes have received, there are few instances where their assembly and disassembly can be triggered over a short time scale and the consequences for the cell assessed. Our data support the idea that podosomes enhance DC migration through three-dimensional space and that their TLR ligand-induced loss might aid local antigen capture by transiently arresting migration. Moreover, we show that MT1-MMP activity is organized by DC podosomes for pericellular proteolysis but that a distinct MMP activity, ADAM17, is involved in their TLR ligand–triggered disassembly. Taken as a whole, these data reveal new features of podosomes and suggest they play an important role in the early DC response to innate immune stimuli.

Materials and methods

Dendritic cell culture

DC were cultured from mouse bone marrow (BMDC) or spleen (SDC) from female C57/Bl6, C3H/HeJ, or C3H/HeN mice, as described previously (West et al., 2004). In brief, bone marrow was flushed from femurs and tibia, and cells were cultured in complete RPMI containing 10 ng/ml recombinant granulocyte macrophage colony–stimulating factor (GM-CSF; PeproTech). The medium was replaced on day three of culture and the cells were used between days five and seven. For SDC, disaggregated splenocytes were cultured in low-attachment plates (Costar) in complete RPMI medium supplemented with 10 ng/ml GM-CSF and 1 ng/ml TGFβ (R&D Systems). SDC were used between 14 and 21 d of culture. Where indicated, DC were derived from MMP2 (provided by C. Libert, University of Ghent, Ghent, Belgium; Itoh et al., 1997), MMP9 (Z. Werb, University of California, San Francisco, San Francisco, California; Vu et al., 1998), or MT1-MMP (Zhou et al., 2000) knockout mice. $ADAM17^{fl/fl}$ mice were generated by a novel strategy, which induced an aberrant splicing event, and show ~10% of ADAM17 expression and activity as compared with wild-type mice. Using a novel strategy, $ADAM17^{fl/fl}$ mice were generated by introducing into the germ line a new exon between exons 11 and 12 so that the new exon started with a translational stop codon. Because we used splice donor/acceptor sites that deviated slightly from the canonical splice donor/acceptor sequence, the new exon was only used in 90–95% of the transcripts, leaving 5–10% of the ADAM17 mRNAs with the wild-type sequence. These 5–10% were enough for the mice to survive. Consequently, $ADAM17^{fl/fl}$ mice show a 90–95% reduction in ADAM17 expression.

Inhibitors, TLR ligands, and stimuli

MMP inhibitors TAPI-1 (BIOMOL International, L.P.), TAPI-2 (BIOMOL International, L.P.), GM6001 (EMD), and CT1746 (G. Murphy, University of Cambridge, Cambridge, England, UK) were all used at 25 µM. GW280264X and GI254023X were both used at 3 µM. Stimulation was performed with TLR ligands LPS (50 ng/ml; Qbiogene) and Pam3CSK (100 ng/ml; EMC Microcollections), or with PMA (30 ng/ml; Sigma-Aldrich) or PGE_2 (10 µg/ml; Qbiogene).

Light microscopy

For visualization and quantitation of cell adhesions, 2×10^5 DC that had been plated onto glass coverslips were fixed with 4% paraformaldehyde in PBS, permeabilized with 0.2% Triton X-100, and costained with TRITC-phalloidin (Sigma-Aldrich) for F-actin and anti-vinculin (hVin-1; Sigma-Aldrich), followed by Alexa 488– or 633–goat anti–mouse IgG (Invitrogen). Single optical sections of 0.7 µm, taken at the ventral surface of the cells, were acquired on a confocal microscope (LSM 510 META) using a 100× α PlanFluar/NA 1.45 objective and LSM 510 software (all from Carl Zeiss, Inc.). Time-lapse video microscopy of BMDC expressing GFP-actin was performed using a 37°C temperature-controlled chamber flushed with 5% CO_2 in air, and images were collected using the microscope and objective as before. For matrix degradation, z stacks of 10 × 0.7-µm sections were acquired every 2 min, taken at 0.34-µm intervals. For each time point, the stacks were converted into a single projection using software (Carl Zeiss, Inc.), and the time series was converted into a QuickTime video (Apple). For analysis of podosome lifetimes, 5 × 0.7-µm sections at 0.34-µm intervals were acquired every 20 s. Maximum projections for each z series, for 50 sequential frames, were imported into the Imaris software (Bitplane AG) for analysis as described in the following section.

Quantitation

Quantitation of the percentage of cells with podosomes or with focal contacts was performed using cells stained with TRITC-phalloidin and anti-vinculin. 200–300 cells per condition per experiment were assessed for podosomes and 150–200 for focal contacts.

For quantitation of the number of focal contacts or of the ventral cell surface area, images collected using identical acquisition parameters were analyzed using Volocity software (PerkinElmer). Focal contacts were selected by intensity of green fluorescence (vinculin) and distinguished from podosomes based on size. The total number of focal contacts for individual complete cells (defined by regions of interest) in each image was then calculated. For measurement of the ventral surface areas, all of the cells in an image were first identified by fluorescence in the red channel (TRITC-phalloidin staining of cortical actin). This selected the precise area of the cells. To extract this data for individual cells in the field, each complete cell was selected using a simple region of interest. The mean area per cell for each condition was then calculated.

For measurement of podosome lifetimes, time sequences were analyzed using Imaris software by a modification of the methods of Evans et al. (2003). In brief, the time sequences were converted to kymographs by swapping time for z and filtered to remove background fluorescence and noise. The images were then cut into uniformly sampled yz slices of 10 pixels, with 5-pixel intervals between the slices, starting at a random point (see Fig. S3). All podosome lives in the kymographs slices were measured regardless of whether they originated outside the time window or continued beyond this window. The total lifetime for all podosomes scored in these cell slices was then divided by the total number of podosome initiation events to give the mean podosome lifetime for each cell.

Transwell migration

BMDC from C3H/HeN or C3H/HeJ mice were labeled with 0.2 µM carboxyfluorescein succinimidyl ester (CFSE) or 2 µM CMTMR (Invitrogen) for 15 min at 37°C, washed three times, and then reincubated for a further 15 min at 37°C. The two populations of cells were mixed in a 1:1 ratio, and 10^5 mixed cells were placed in the upper chamber of a Transwell 24-well insert (5-µm pore filter; Costar) or directly into the well without an insert (input control). After 2 h at 37°C, the cells that had migrated through the filter were recovered using 10 mM EDTA and stained with an APC-labeled anti-CD11c antibody (HL3; BD Biosciences). Then, the ratio of CFSE- to CMTMR-labeled $CD11c^+$ cells was assessed by flow cytometry using a FACS Calibur (BD Biosciences). Where indicated, DC were pretreated with 50 ng/ml LPS before migration. To normalize the data across a time course, the ratio of migrated HeN/HeJ cells was divided by the input ratio for each time point.

Matrix degradation

Glass coverslips were coated with matrix proteins: 10 µg/ml FITC-gelatin (Invitrogen), 10 µg/ml Alexa 594–gelatin, 50 µg/ml Oregon green–collagen

type IV (Invitrogen), or 50 µg/ml Alexa 488–fibronectin and cross-linked with 0.5% glutaraldehyde where indicated (Bowden et al., 2001). Labeling of gelatin (Sigma-Aldrich) and fibronectin (EMD) with Alexa 594 and 488 dyes was performed using the respective protein labeling kits (Invitrogen) according to the manufacturer's instructions. 2×10^5 DC were plated onto matrix-coated coverslips and incubated at 37°C to allow degradation, then fixed with 4% paraformaldehyde in PBS and stained with TRITC-phalloidin. Matrix degradation was quantitated by counting degradation patches in 15 fields of cells (300–500 cells) per condition for each experiment. For time-lapse analysis of matrix degradation, BMDC infected with retrovirus expressing GFP-actin were plated into glass-bottomed dishes (WillCo; Intracel) coated with cross-linked Alexa 594–gelatin.

FITC-dextran uptake

2×10^5 SDC that had been allowed to adhere to glass coverslips for 1–2 h were pretreated with 25 µM TAPI-1, then stimulated with 100 ng/ml Pam3CSK for 30 min before incubation with 1 mg/ml FITC-dextran (Invitrogen) for 10 min at 37°C. Cells were detached with PBS containing 5 mM EDTA, and pinocytosed dextran was measured by flow cytometry (West et al., 2004).

Retroviral constructs and BMDC retroviral infection

Mouse ADAM17 cDNA (Thermo Fisher Scientific) was cloned into the BamHI and XhoI sites of the Moloney murine leukemia virus–based vector pBMN-IRES-GFP (provided by G. Nolan, Stanford University, Stanford, CA). LZRS-pBMN EGFP-actin has been described previously (West et al., 2004). Virus was produced by transfecting the Phoenix Eco 293T packaging cell line with these vectors, and BMDC were infected using viral supernatants as described previously (West et al., 2004).

TNF-α shedding

10^5 DC were plated into 96-well plates in 100 µl of complete RPMI and stimulated with 50 ng/ml LPS or 100 ng/ml Pam3CSK for 2 h, then 10 µl of the medium was assayed for secreted TNF-α by ELISA (Peprotech), according to the manufacturer's instructions.

Cell lysis and immunoblot

DC were lysed in SDS sample buffer. Equal amounts of proteins were separated by electrophoresis on 4–12% NuPage gels (Invitrogen), then transferred onto nitrocellulose membrane (GE Healthcare) and probed with antibodies against ADAM17 (Spring Bioscience) and actin (AC-40; Sigma-Aldrich).

Statistical analysis

Error bars represent SEM unless otherwise stated. The unpaired two-tailed *t* test was used for statistical analysis.

Online supplemental material

Fig. S1 shows that DC from C3H/HeJ mice are insensitive to LPS stimulation of FITC-dextran pinocytosis or podosome disassembly. Fig. S2 shows podosome-associated degradation of gelatin, collagen type IV, and fibronectin. Fig. S3 illustrates the method used for measurement of podosome lifetimes. Video 1 shows spreading, ruffling, and pinocytosis in DC in response to LPS treatment. Video 2 shows degradation of gelatin matrix by DC expressing GFP-actin. Online supplemental material is available at http://www.jcb.org/cgi/content/full/jcb.200801022/DC1.

We thank Gill Murphy and colleagues for generous provision of reagents and advice, Dylan Edwards for quantitative MMP expression analysis, Claude Libert and Zena Werb for cells from MMP2- and MMP9-deficient mice, Rossana Zaru and Christian Gawden-Bone for discussions, and Pamela Mollahan for GFP-actin retrovirus production.

We are grateful to the Medical Research Council for program grant GO200536 (to C. Watts and A.R. Prescott) and the Hong Kong Research Grant Council (grant CERG 751303 to Z. Zhou) for funding.

Submitted: 7 January 2008
Accepted: 4 August 2008

References

Black, R.A., C.T. Rauch, C.J. Kozlosky, J.J. Peschon, J.L. Slack, M.F. Wolfson, B.J. Castner, K.L. Stocking, P. Reddy, S. Srinivasan, et al. 1997. A metalloproteinase disintegrin that releases tumour-necrosis factor-alpha from cells. *Nature.* 385:729–733.

Blander, J.M., and R. Medzhitov. 2004. Regulation of phagosome maturation by signals from toll-like receptors. *Science.* 304:1014–1018.

Blander, J.M., and R. Medzhitov. 2006. Toll-dependent selection of microbial antigens for presentation by dendritic cells. *Nature.* 440:808–812.

Boes, M., N. Bertho, J. Cerny, M. Op den Brouw, T. Kirchhausen, and H. Ploegh. 2003. T cells induce extended class II MHC compartments in dendritic cells in a toll-like receptor-dependent manner. *J. Immunol.* 171:4081–4088.

Bowden, E.T., P.J. Coopman, and S.C. Mueller. 2001. Invadopodia: unique methods for measurement of extracellular matrix degradation in vitro. *Methods Cell Biol.* 63:613–627.

Buccione, R., J.D. Orth, and M.A. McNiven. 2004. Foot and mouth: podosomes, invadopodia and circular dorsal ruffles. *Nat. Rev. Mol. Cell Biol.* 5:647–657.

Burns, S., A.J. Thrasher, M.P. Blundell, L. Machesky, and G.E. Jones. 2001. Configuration of human dendritic cell cytoskeleton by Rho GTPases, the WAS protein, and differentiation. *Blood.* 98:1142–1149.

Burns, S., S.J. Hardy, J. Buddle, K.L. Yong, G.E. Jones, and A.J. Thrasher. 2004. Maturation of DC is associated with changes in motile characteristics and adherence. *Cell Motil. Cytoskeleton.* 57:118–132.

Calle, Y., N.O. Carragher, A.J. Thrasher, and G.E. Jones. 2006. Inhibition of calpain stabilises podosomes and impairs dendritic cell motility. *J. Cell Sci.* 119:2375–2385.

Chalaris, A., B. Rabe, K. Paliga, H. Lange, T. Laskay, C.A. Fielding, S.A. Jones, S. Rose-John, and J. Scheller. 2007. Apoptosis is a natural stimulus of IL6R shedding and contributes to the proinflammatory trans-signaling function of neutrophils. *Blood.* 110:1748–1755.

Chou, H.C., I.M. Anton, M.R. Holt, C. Curcio, S. Lanzardo, A. Worth, S. Burns, A.J. Thrasher, G.E. Jones, and Y. Calle. 2006. WIP regulates the stability and localization of WASP to podosomes in migrating dendritic cells. *Curr. Biol.* 16:2337–2344.

Chow, A., D. Toomre, W. Garrett, and I. Mellman. 2002. Dendritic cell maturation triggers retrograde MHC class II transport from lysosomes to the plasma membrane. *Nature.* 418:988–994.

Destaing, O., F. Saltel, J.C. Geminard, P. Jurdic, and F. Bard. 2003. Podosomes display actin turnover and dynamic self-organization in osteoclasts expressing actin-green fluorescent protein. *Mol. Biol. Cell.* 14:407–416.

Endo, K., T. Takino, H. Miyamori, H. Kinsen, T. Yoshizaki, M. Furukawa, and H. Sato. 2003. Cleavage of syndecan-1 by membrane type matrix metalloproteinase-1 stimulates cell migration. *J. Biol. Chem.* 278:40764–40770.

Evans, J.G., I. Correia, O. Krasavina, N. Watson, and P. Matsudaira. 2003. Macrophage podosomes assemble at the leading lamella by growth and fragmentation. *J. Cell Biol.* 161:697–705.

Granucci, F., E. Ferrero, M. Foti, D. Aggujaro, K. Vettoretto, and P. Ricciardi-Castagnoli. 1999. Early events in dendritic cell maturation induced by LPS. *Microbes Infect.* 1:1079–1084.

Guermonprez, P., J. Valladeau, L. Zitvogel, C. Thery, and S. Amigorena. 2002. Antigen presentation and T cell stimulation by dendritic cells. *Annu. Rev. Immunol.* 20:621–667.

Heath, W.R., and F.R. Carbone. 2001. Cross-presentation, dendritic cells, tolerance and immunity. *Annu. Rev. Immunol.* 19:47–64.

Holmbeck, K., P. Bianco, J. Caterina, S. Yamada, M. Kromer, S.A. Kuznetsov, M. Mankani, P.G. Robey, A.R. Poole, I. Pidoux, et al. 1999. MT1-MMP-deficient mice develop dwarfism, osteopenia, arthritis, and connective tissue disease due to inadequate collagen turnover. *Cell.* 99:81–92.

Huang, F.P., N. Platt, M. Wykes, J.R. Major, T.J. Powell, C.D. Jenkins, and G.G. MacPherson. 2000. A discrete subpopulation of dendritic cells transports apoptotic intestinal epithelial cells to T cell areas of mesenteric lymph nodes. *J. Exp. Med.* 191:435–444.

Hundhausen, C., D. Misztela, T.A. Berkhout, N. Broadway, P. Saftig, K. Reiss, D. Hartmann, F. Fahrenholz, R. Postina, V. Matthews, et al. 2003. The disintegrin-like metalloproteinase ADAM10 is involved in constitutive cleavage of CX3CL1 (fractalkine) and regulates CX3CL1-mediated cell-cell adhesion. *Blood.* 102:1186–1195.

Itoh, T., T. Ikeda, H. Gomi, S. Nakao, T. Suzuki, and S. Itohara. 1997. Unaltered secretion of beta-amyloid precursor protein in gelatinase A (matrix metalloproteinase 2)-deficient mice. *J. Biol. Chem.* 272:22389–22392.

Kleijmeer, M., G. Ramm, D. Schuurhuis, J. Griffith, M. Rescigno, P. Ricciardi-Castagnoli, A.Y. Rudensky, F. Ossendorp, C.J. Melief, W. Stoorvogel, and H.J. Geuze. 2001. Reorganization of multivesicular bodies regulates MHC class II antigen presentation by dendritic cells. *J. Cell Biol.* 155:53–63.

Lanzavecchia, A., and F. Sallusto. 2001. Regulation of t cell immunity by dendritic cells. *Cell.* 106:263–266.

Lelouard, H., E. Gatti, F. Cappello, O. Gresser, V. Camosseto, and P. Pierre. 2002. Transient aggregation of ubiquitinated proteins during dendritic cell maturation. *Nature.* 417:177–182.

Linder, S. 2007. The matrix corroded: podosomes and invadopodia in extracellular matrix degradation. *Trends Cell Biol.* 17:107–117.

Linder, S., and M. Aepfelbacher. 2003. Podosomes: adhesion hot-spots of invasive cells. *Trends Cell Biol.* 13:376–385.

Mott, J.D., and Z. Werb. 2004. Regulation of matrix biology by matrix metalloproteinases. *Curr. Opin. Cell Biol.* 16:558–564.

Nakahara, H., L. Howard, E.W. Thompson, H. Sato, M. Seiki, Y. Yeh, and W.T. Chen. 1997. Transmembrane/cytoplasmic domain-mediated membrane type 1-matrix metalloprotease docking to invadopodia is required for cell invasion. *Proc. Natl. Acad. Sci. USA.* 94:7959–7964.

Nakamura, H., N. Suenaga, K. Taniwaki, H. Matsuki, K. Yonezawa, M. Fujii, Y. Okada, and M. Seiki. 2004. Constitutive and induced CD44 shedding by ADAM-like proteases and membrane-type 1 matrix metalloproteinase. *Cancer Res.* 64:876–882.

Poltorak, A., X. He, I. Smirnova, M.Y. Liu, C. Van Huffel, X. Du, D. Birdwell, E. Alejos, M. Silva, C. Galanos, et al. 1998. Defective LPS signaling in C3H/HeJ and C57BL/10ScCr mice: mutations in Tlr4 gene. *Science.* 282:2085–2088.

Ratzinger, G., P. Stoitzner, S. Ebner, M.B. Lutz, G.T. Layton, C. Rainer, R.M. Senior, J.M. Shipley, P. Fritsch, G. Schuler, and N. Romani. 2002. Matrix metalloproteinases 9 and 2 are necessary for the migration of Langerhans cells and dermal dendritic cells from human and murine skin. *J. Immunol.* 168:4361–4371.

Reis e Sousa, C. 2006. Dendritic cells in a mature age. *Nat. Rev. Immunol.* 6:476–483.

Ridley, A.J., M.A. Schwartz, K. Burridge, R.A. Firtel, M.H. Ginsberg, G. Borisy, J.T. Parsons, and A.R. Horwitz. 2003. Cell migration: integrating signals from front to back. *Science.* 302:1704–1709.

Rousseau, S., M. Papoutsopoulou, A. Symons, D. Cook, J.M. Lucocq, A.R. Prescott, A. O'Garra, S.C. Ley, and P. Cohen. 2008. TPL2-mediated activation of ERK1 and ERK2 regulates the processing of pre-TNF alpha in LPS-stimulated macrophages. *J. Cell Sci.* 121:149–154.

Sallusto, F., and A. Lanzavecchia. 2000. Understanding dendritic cell and T-lymphocyte traffic through the analysis of chemokine receptor expression. *Immunol. Rev.* 177:134–140.

Saltel, F., A. Chabadel, E. Bonnelye, and P. Jurdic. 2008. Actin cytoskeletal organisation in osteoclasts: A model to decipher transmigration and matrix degradation. *Eur. J. Cell Biol.* 87:459–468.

Sato, H., T. Takino, and H. Miyamori. 2005. Roles of membrane-type matrix metalloproteinase-1 in tumor invasion and metastasis. *Cancer Sci.* 96:212–217.

Schlondorff, J., and C.P. Blobel. 1999. Metalloprotease-disintegrins: modular proteins capable of promoting cell-cell interactions and triggering signals by protein-ectodomain shedding. *J. Cell Sci.* 112:3603–3617.

Seals, D.F., and S.A. Courtneidge. 2003. The ADAMs family of metalloproteases: multidomain proteins with multiple functions. *Genes Dev.* 17:7–30.

Shin, J.S., M. Ebersold, M. Pypaert, L. Delamarre, A. Hartley, and I. Mellman. 2006. Surface expression of MHC class II in dendritic cells is controlled by regulated ubiquitination. *Nature.* 444:115–118.

Soond, S.M., B. Everson, D.W. Riches, and G. Murphy. 2005. ERK-mediated phosphorylation of Thr735 in TNFalpha-converting enzyme and its potential role in TACE protein trafficking. *J. Cell Sci.* 118:2371–2380.

Steinman, R.M., D. Hawiger, and M.C. Nussenzweig. 2003. Tolerogenic dendritic cells. *Annu. Rev. Immunol.* 21:685–711.

Svensson, H.G., M.A. West, P. Mollahan, A.R. Prescott, R. Zaru, and C. Watts. 2008. A role for ARF6 in dendritic cell podosome formation and migration. *Eur. J. Immunol.* 38:818–828.

Trombetta, E.S., and I. Mellman. 2005. Cell biology of antigen processing in vitro and in vivo. *Annu. Rev. Immunol.* 23:975–1028.

Trombetta, E.S., M. Ebersold, W. Garrett, M. Pypaert, and I. Mellman. 2003. Activation of lysosomal function during dendritic cell maturation. *Science.* 299:1400–1403.

van Helden, S.F., D.J. Krooshoop, K.C. Broers, R.A. Raymakers, C.G. Figdor, and F.N. van Leeuwen. 2006. A critical role for prostaglandin E2 in podosome dissolution and induction of high-speed migration during dendritic cell maturation. *J. Immunol.* 177:1567–1574.

van Helden, S.F., M.M. Oud, B. Joosten, N. Peterse, C.G. Figdor, and F.N. van Leeuwen. 2008. PGE2-mediated podosome loss in dendritic cells is dependent on actomyosin contraction downstream of the RhoA-Rho-kinase axis. *J. Cell Sci.* 121:1096–1106.

Van Lint, P., and C. Libert. 2007. Chemokine and cytokine processing by matrix metalloproteinases and its effect on leukocyte migration and inflammation. *J. Leukoc. Biol.* 82:1375–1381.

van Niel, G., R. Wubbolts, T. Ten Broeke, S.I. Buschow, F.A. Ossendorp, C.J. Melief, G. Raposo, B.W. van Balkom, and W. Stoorvogel. 2006. Dendritic cells regulate exposure of MHC class II at their plasma membrane by oligoubiquitination. *Immunity.* 25:885–894.

Vu, T.H., J.M. Shipley, G. Bergers, J.E. Berger, J.A. Helms, D. Hanahan, S.D. Shapiro, R.M. Senior, and Z. Werb. 1998. MMP-9/gelatinase B is a key regulator of growth plate angiogenesis and apoptosis of hypertrophic chondrocytes. *Cell.* 93:411–422.

Watts, C., R. Zaru, A.R. Prescott, R.P. Wallin, and M.A. West. 2007. Proximal effects of Toll-like receptor activation in dendritic cells. *Curr. Opin. Immunol.* 19:73–78.

West, M.A., R.P. Wallin, S.P. Matthews, H.G. Svensson, R. Zaru, H.G. Ljunggren, A.R. Prescott, and C. Watts. 2004. Enhanced dendritic cell antigen capture via toll-like receptor-induced actin remodeling. *Science.* 305:1153–1157.

Wheeler, A.P., C.M. Wells, S.D. Smith, F.M. Vega, R.B. Henderson, V.L. Tybulewicz, and A.J. Ridley. 2006. Rac1 and Rac2 regulate macrophage morphology but are not essential for migration. *J. Cell Sci.* 119:2749–2757.

Wilson, N.S., and J.A. Villadangos. 2005. Regulation of antigen presentation and cross-presentation in the dendritic cell network: facts, hypothesis, and immunological implications. *Adv. Immunol.* 86:241–305.

Zhou, Z., S.S. Apte, R. Soininen, R. Cao, G.Y. Baaklini, R.W. Rauser, J. Wang, Y. Cao, and K. Tryggvason. 2000. Impaired endochondral ossification and angiogenesis in mice deficient in membrane-type matrix metalloproteinase I. *Proc. Natl. Acad. Sci. USA.* 97:4052–4057.